Available online at www.sciencedirect.com
ScienceDirect
Journal of Power Sources 162 (2006) 679–684
JOURNAL OF POWER SOURCES
www.elsevier.com/locate/jpowsour

Short communication

Copper–vanadium mixed oxide thin film electrodes

E.A. Souza [a], A.O. dos Santos [a], L.P. Cardoso [a], M.H. Tabacniks [b], R. Landers [a], A. Gorenstein [a,*]

[a] *Applied Physics Department, Physics Institute, UNICAMP, CP 6165, CEP 13083-970 Campinas, SP, Brazil*
[b] *Physics Institute, USP, CP 66318, CEP 05389-970 São Paulo, SP, Brazil*

Received 14 June 2006; received in revised form 4 July 2006; accepted 5 July 2006
Available online 17 August 2006

Abstract

In this work, small amounts of vanadium atoms were incorporated in copper oxide films in order to decrease the charge capacity loss during the electrochemical lithium reaction, mainly in the first cycle. Reactive sputtering was the film deposition technique used to deposit pure copper oxide films, CuO, and copper–vanadium mixed oxides CuO(VO_y). The composition, oxidation state and crystallinity of the deposited films were investigated. Electrochemical studies were performed, and the results demonstrated that the mixed oxides have a better electrochemical behavior with a higher capacity and stability in the charge/discharge processes, when compared to the pure CuO films behavior.

Keywords: Copper oxide; Vanadium; Reactive sputtering; Thin films; Microbatteries; Electrode

1. Introduction

Copper oxide can be found in two different compositions: cupric oxide (Cu_2O), with cubic structure, and cuprous oxide (CuO), which presents monoclinic structure [1,2]. The bulk material density of CuO and Cu_2O is 6.3 and 6.0 g cm^{-3}, respectively [3].

In the battery field, copper oxide has been used as cathode material in primary lithium batteries [4,5], due to its high specific capacity. Li/CuO cells present an energy density of 600 Wh dm^{-3} (300 Wh kg^{-1}) and a theoretical capacity of 4.26 Ah cm^{-3} (670 mAh g^{-1}). The open circuit potential is 2.25 V and the cell operates in an average potential between 1.2 and 1.5 V [4,5]. Copper oxide presents high stability in organic electrolytes, due to its low solubility [6]. This characteristic assures a low self-discharge (<1% per year at ambient temperature) allowing a long shelf life [4,6].

Recently [7–9], it was demonstrated that copper oxide, both in powder (CuO and Cu_2O) and in thin film form (CuO), is capable of react with lithium ions in a reversible way, and is a viable material to be used as electrode in rechargeable lithium batteries. However, the material presents a large capacity loss from the first to the second discharge cycle [7,9,10].

In this work, small amounts of vanadium atoms were incorporated in copper oxide films during the film deposition process, in order to decrease the initial charge capacity loss, and to increase the coulombic efficiency of the lithium reaction process during the successive cycles.

2. Experimental

The oxide films were deposited by d.c. and r.f. sputtering from a copper and vanadium targets, respectively, in an O_2 + Ar atmosphere. The flow of the gases was controlled by two mass flowmeters, and was fixed at 55.0 sccm (Ar) and 5.0 sccm (O_2). The pressure under deposition was 1.0×10^{-2} mbar. A diagram of the sputtering chamber is shown in Fig. 1. The target to substrate distance was ~13 cm. The support of the d.c. target was inclined at 13° due to the position of the substrate on the sample holder. The target diameter (V and Cu) was 5.0 cm. The substrates were indium–tin oxide (ITO, used in electrochemical and X-ray Photoelectron Spectroscopy measurements), glass (used in the X-ray diffraction experiments), carbon or silicon (used in the Rutherford Scattering Spectroscopy experiments). A small part of the substrate was covered with adhesive tape, in order to provide a well-defined step. This step was used in the thickness measurements, by means of an Alpha-Step profilometer.

The presence of crystalline phases was investigated by X-ray diffraction with Cu Kα radiation either under grazing incidence

* Corresponding author. Tel.: +55 19 37885411; fax: +55 19 37885376.
E-mail address: annette@ifi.unicamp.br (A. Gorenstein).

0378-7753/$ – see front matter © 2006 Elsevier B.V. All rights reserved.
doi:10.1016/j.jpowsour.2006.07.011

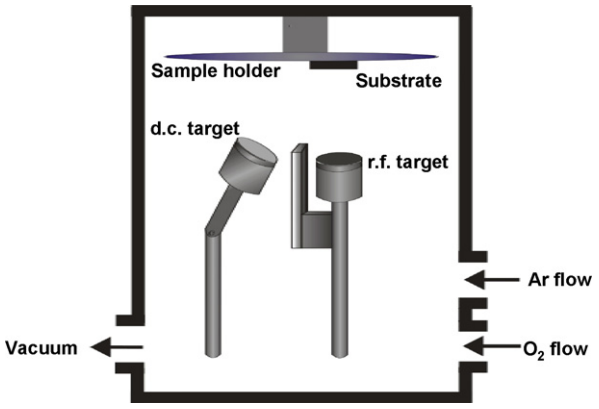

Fig. 1. Diagram of the sputtering chamber geometry.

geometry in the X Pert MRD Philips equipment or in diffractograms with Fe Kα radiation and a graphite monochromator, in a Theta-2Theta Bragg–Brentano geometry. Cu, V and O contents were obtained by Rutherford Back Scattering (RBS) Spectroscopy using a 2.2 MeV He^+ beam.

The chemical state of the metals was analyzed by X-ray Absorption Near-edge Structure (XANES). The experiments were performed at the XAS beamline (LNLS—Laboratório Nacional de Luz Síncrotron, Campinas, SP). The photon energy was in the range 8900–9100 eV (copper absorption K-edge) or 5380–5600 eV (vanadium absorption K-edge). The thin film samples were analyzed in the fluorescence mode, and the control samples.

(CuO and V_2O_5 pellets) were measured in transmission mode. The chemical state of the elements was also analyzed by X-ray Photoelectron Spectroscopy (XPS).

Electrochemical cells with the oxide films as the working electrode and two Li metal foils as the reference and counter electrode were used for electrochemical measurements. The electrolyte was 1 M $LiClO_4$ in propylene carbonate. Chronopotentiometric experiments were performed from rest potential to 1 V versus Li, using a current density of 2.0 μA cm^{-2}, by means of a multipotentiostat (VMP system, Biologic) operating in the galvanostatic mode. During the experiments, the cell was maintained inside an Ar dry-box.

3. Results

In this work, copper oxide and mixed vanadium–copper oxides, $Cu_xV_yO_z$, films were deposited and analyzed. The pure copper oxide film (herein called CuV0) was deposited using a d.c. sputtering. The power applied to the copper target was 4 W. For the deposition of mixed oxides this power level at the copper target was maintained and an r.f. sputtering system with a vanadium target was simultaneously actionated. The r.f. power levels were 60, 80 and 100 W, and the obtained thin film samples will be herein denominated CuV60, CuV80 and CuV100, respectively. The composition of all films, deposited onto car-

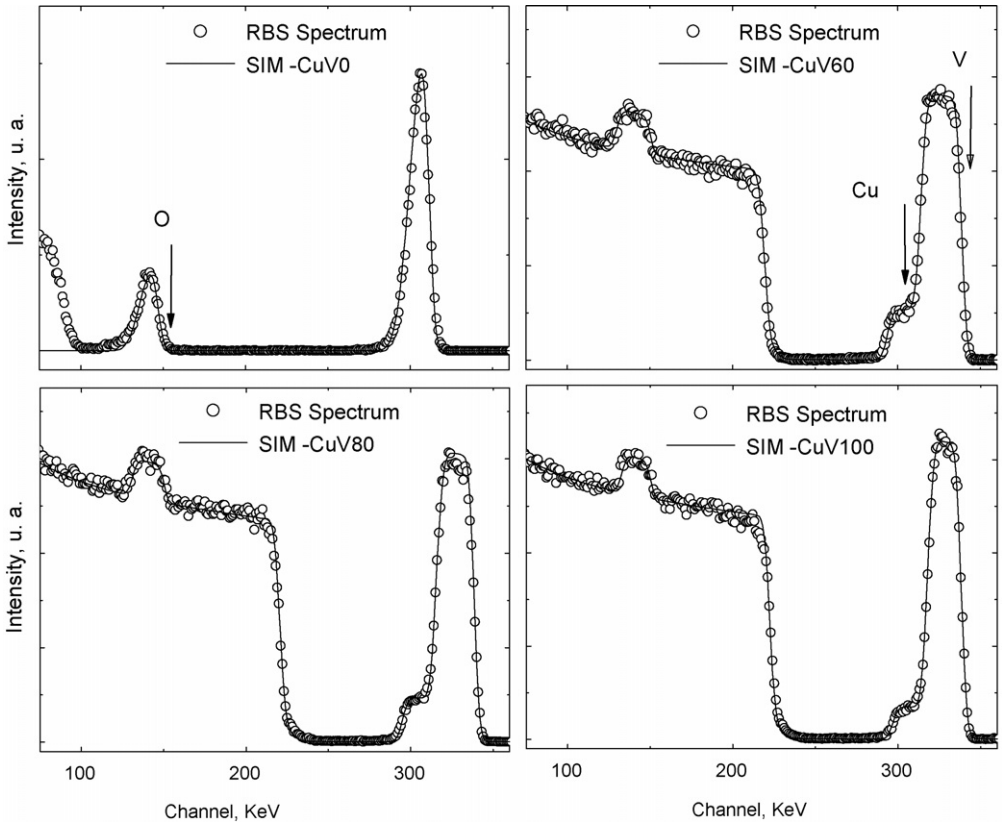

Fig. 2. RBS Spectra and fitting curves. The substrate for films CuV60, CuV80 and CuV100 was Si and for CuV0 film was C.

Table 1
Composition, density and thickness for thin film samples

Sample	Power r.f./d.c.	Composition	Density ($g\,cm^{-3}$)	Thickness (nm)
CuV0	0/4	$CuO_{0.9}$	4.9	116.0
CuV60	60/4	$V_{0.17}CuO_{1.60}$	5.4	97.0
CuV80	80/4	$V_{0.24}CuO_{1.63}$	5.4	119.8
CuV100	100/4	$V_{0.30}CuO_{1.86}$	6.7	121.7

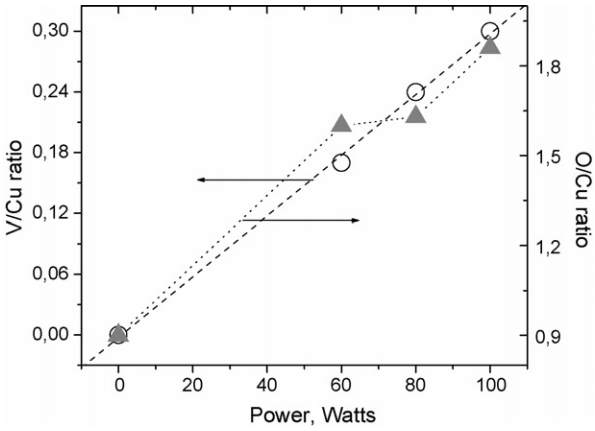

Fig. 3. Vanadium/copper ratio and oxygen/copper vs. applied r.f. power.

bon or silicon substrates, was determined by simulating the RBS spectra (Fig. 2), using the software RUMP [11]. These results, as well as the measured thickness and the calculated density are presented in Table 1.

There is a linear relationship between the vanadium/copper ratio content and the applied r.f. power (Fig. 3). In what concerns the oxide formation, the sample deposited without vanadium can be considered a cuprous oxide sample, with a small oxygen deficiency.

The next sample in the series (CuV60) has the composition $V_{0.17}CuO_{1.60}$. The insertion of vanadium in the copper oxide is accompanied by an important increase in the relative oxygen content (Fig. 3), which is an indication of vanadium oxide formation. With the increase of the power applied to the vanadium target from 60 to 80 W (sample CuV80), the relative oxygen content in the sample does not increase. The O/Cu ratio and the density (Fig. 3 and Table 1) does not change indicating that the sample CuV80 has either a less compact structure or presents a higher porosity if compared to sample CuV60. For the last sample in the series (CuV100) both the O/Cu ratio and the density increase.

The copper K-edge spectra obtained from the XANES experiments are presented in Fig. 4. All graphs presented an intense energy band at 8996.2 eV. This band is characteristic of copper with oxidation state +2 and is attributed to electronic transitions from 1s to 4p [12,13]. The shakedown transitions (shoulder presented at 8986.2 eV) were intense only for the film deposited without vanadium (sample CuV0) [14]. The intensity of these transitions is related to the presence of holes in O2p orbital (the increase on the amount of holes in these orbital implies a decrease in the intensity). Then, the decrease of the intensity of these transitions in mixed oxides is a direct consequence of the increase in the oxygen content [15].

The vanadium K-edge spectra obtained from the XANES experiments are presented in Fig. 5 (samples CuV60, CuV80, CuV100 and V_2O_5 control sample). The XANES profile is very similar to the one found for vitreous compounds, in which vanadium is present in the oxidation state +5 [16]. In these compounds, the pre-peak is located at 5470 eV, and just after the edge a peak superposition forms a large band ~5509 eV [16]. For thin film compounds, this observed value is ~5508 eV. In our case, the peak located in the pre-edge region is shifted to regions of lower energies (5469.1 eV), if compared to the control sample V_2O_5. The shift of these peaks could be an indication of the existence of vanadium in oxidation states lower than +5 [12,16]; this, however, was not confirmed by XPS, as discussed in the following.

The XPS analysis was performed only in the sample CuV100. The V2p and O1s lines were analyzed by adjusting the spectrum with a gaussian function. The results (peak position and full-width at half-maximum, FWHM) are presented in Table 2.

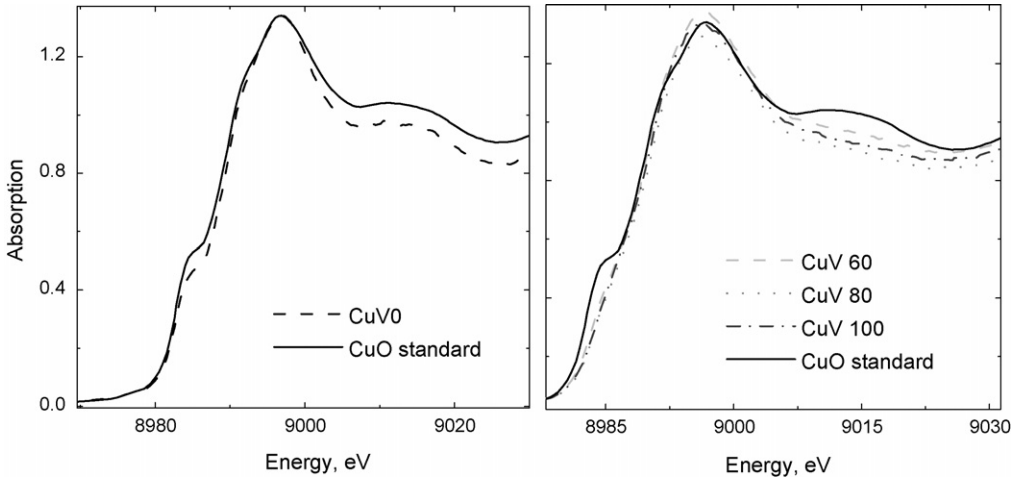

Fig. 4. Copper K-edge XANES spectra for all samples. The spectrum for the standard CuO pellet is also presented.

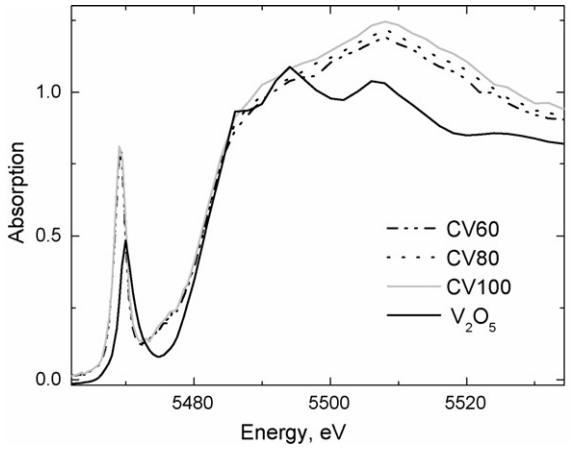

Fig. 5. Vanadium K-edge XANES spectra for all samples. The spectrum for the standard V_2O_5 pellet is also presented.

Table 2
Peak positions and FWHM obtained from the XPS spectra

Sample	Spectral line	Center (eV)	FWHM (eV)
CuV100	$V2p_{3/2}$	516.5	2.0
($V_{0.30}CuO_{1.86}$)	O1s	530.0; 532.4	2.4; 2.5

The spectrum corresponding to the $V2p_{3/2}$ line (Fig. 6) presents only one binding energy, at 516.5 eV and a FWHM of 2.0 eV. These values are a clear indication of the presence of V^{5+} [17,18]. The O1s line could be adjusted with two gaussians, with peak positions at 530.0 and 532.4 eV (Table 2). The energy presented by the first peak, 530.0 eV, can be associated to the photoelectric emissions arising from the oxygen present in the oxide (oxygen bonding in copper oxide and vanadium oxide) [17,19–21], since at the best of our knowledge it does not exist any reported values of O1s signal in these oxides with energies greater than 532 eV. However, the presence of a shoulder with energies values similar to the one observed in the present work has been pointed out in other works concerning ternary oxides ($M_xV_yO_z$) with vanadium [22,23]. Then, the peak located at 532.4 eV could be related to specific bonding

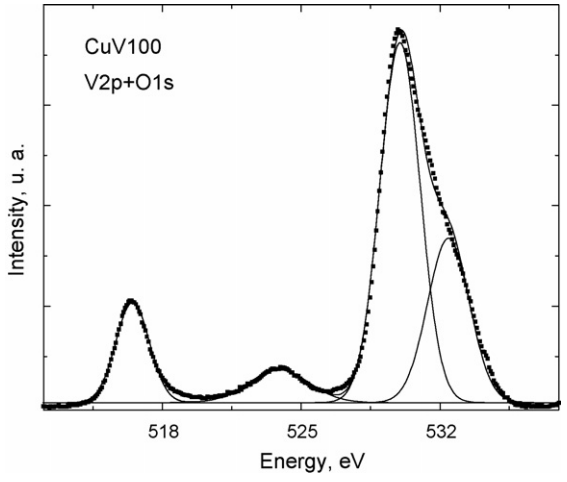

Fig. 6. XPS spectrum (V2p + O1s) for sample CuV100.

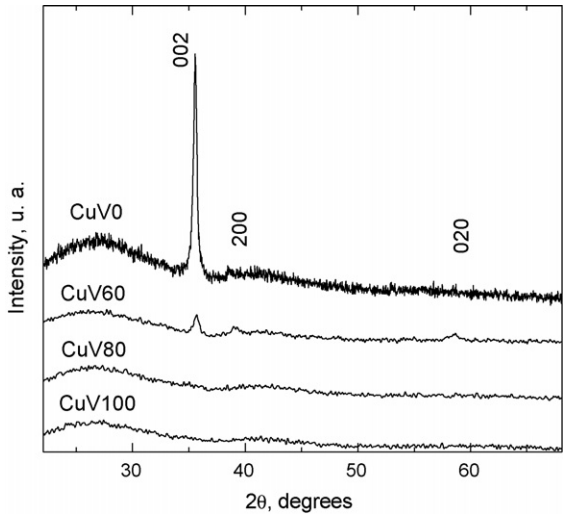

Fig. 7. XRD patterns. Samples were deposited onto glass substrate.

linked to vanadium, being peculiar to the formation of mixed oxides.

Fig. 7 presents the XRD results for all films. Samples CuV0 and CuV60 are polycrystalline; samples CuV80 and CuV100 are amorphous, indicating that the increase of vanadium content caused a decrease in the crystallinity of the films. From these data, it was possible to identify that CuV0 has the expected monoclinic structure, with preferential orientation to the plane (0 0 2). The next sample in the series (CuV60) also has a monoclinic structure but without a preferential orientation (Fig. 7). The main conclusion from the XRD data is that the original structure of CuO is progressively deformed with the inclusion of vanadium. The film became amorphous because the copper oxide structure does not allow the inclusion of foreign atoms, neither in a substitutional nor in interstitial position. The vanadium inclusion deforms the structure, and this deformation is accompanied by the reduction of size of the crystalline grains and general amorphization of the material.

Galvanostatic measurements with current density of 2 $\mu Ah\,cm^{-2}$ were performed. Fig. 8 presents the potential versus composition curve, for the first discharge process. All films have almost the same open circuit potential (~3.6 V versus Li) and an important ohmic drop at the beginning of the cathodic process.

For all films, two discharge plateaus are observed in the first discharge cycle. For the copper oxide film (sample CuV0) the plateaus are located at the potentials 2.3 and 1.4 V versus Li. The electrochemical behavior of copper oxide in lithium-containing electrolytes has been extensively studied [7–9,24,25], but the reaction scheme is still controversial. In a recent work, it was suggested that the first plateau is related to the gradual reduction of Cu(II) in Cu(I) and oxygen vacancies creation. Several authors [24,25] agree that the 1.4 V versus Li plateau arises from the reduction of copper oxide into copper nanograins and formation of Li_2O. For the samples with vanadium inclusion (CuV60, CuV80 and CuV100) the first plateau is located ~2.5 V versus Li. This plateau, for the CuV60 sample, corresponds to a

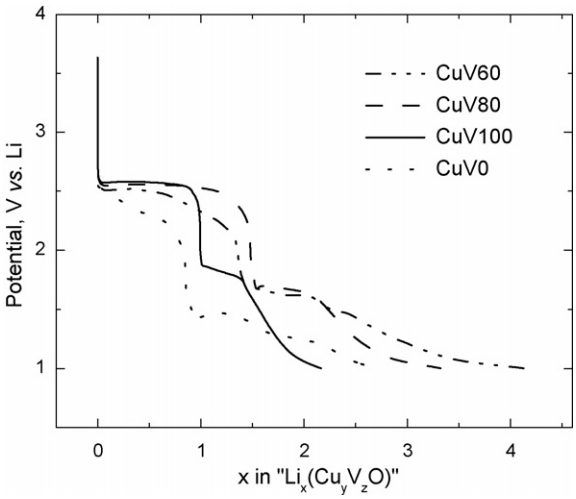

Fig. 8. Voltage–composition curves, for the first discharge process. Samples were deposited onto ITO-covered glass substrate.

lithium uptake of ∼0.5 Li ions per mole of compound. In the potential range from open circuit to 2.0 V versus Li this sample reacts with 1.3 Li ions per mole of compound. As the vanadium content increases, this plateau become more defined, and shows a maximum extension for the film CuV80 (lithium uptake of ∼1.3 Li ions per mole of compound). For the sample with maximum vanadium content, the first plateau corresponds to a lithium uptake of ∼0.9 Li ions per mole of compound. The second plateau, for all samples with vanadium inclusion, is located at ∼1.7 V versus Li, and the extension is independent of the vanadium content. These data indicates that the vanadium reduction occurs since the beginning of the cathodic reaction, simultaneously to the copper reduction. Due to the complexity of the system, it is not an easy task to associate electrochemical reactions to the observed plateaus. The curves are very similar to the ones observed for other mixed oxides [26].

In Fig. 9, the volumetric discharge capacity as a function of cycle number is presented. As already commented in the introduction, the copper oxide presents a strong loss in its ability to react with lithium ions in the second cycle. This loss is probably due to the strong structural changes and the formation of new compounds (metallic copper and lithium oxide) during the discharge process [7]. The inset in Fig. 9 shows the capacity loss for the first cycle as a function of the V/Cu ratio. The initial capacity loss was almost 3 times lower for the mixed oxides; showing that the inclusion of vanadium is beneficial. The sample with the lowest Cu/V ratio was the one that presented the highest volumetric charge capacity in the first cycle (∼563 μAh cm^{-2} μm^{-1} or 1042 mAh g^{-1}), corresponding to ∼4.2 lithium ions per compound molecule. Also, it is interesting to observe the great increase in capacity provoked by the small increase of vanadium in the film CuV60 if compared to the CuV0 film. However, for the other samples in the series, as the vanadium amount in the film increased, the capacity (first cycle) decreased, being 474 μAh cm^{-2} μm^{-1} or 878 mAh g^{-1} (3.2 lithium ions per compound molecule) for the CuV80 film and 358 μAh cm^{-2} μm^{-1} or 533.6 mAh g^{-1} (2.2 lithium ions per compound molecule) for the CuV100 film. It is probable that at the end of the discharge cycle for these samples, metallic copper is formed [25,27,28]. It can also be observed in Fig. 9 that the films containing vanadium presented a lower decrease in discharge capacity. The CuV0 film lose 46.4% of its capacity, the CuV60 and CuV80 films lose less than 14% and the CuV100 film lose 18.0% in the second discharge. The different behavior of the capacity on cycling could be related to the decrease of the crystalline grain size. In other works, it has been observed that during the reduction process the original grains are subdivided into smaller grains. It allows a better reactivity of the metallic copper and the lithium oxide (also formed during the reduction process) during the oxidation process, increasing the efficiency of this electrode in the charge and discharge cycles [7,27].

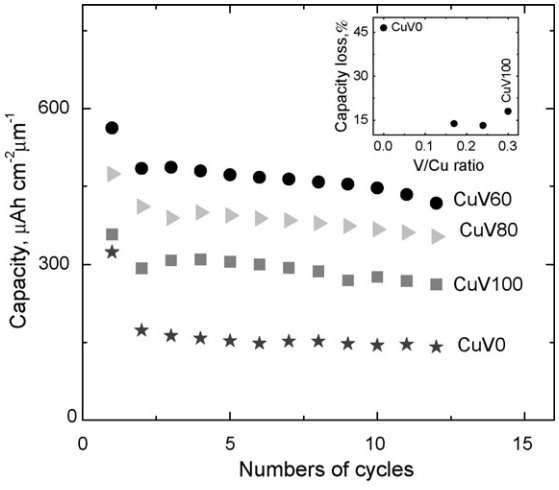

Fig. 9. Discharge capacity as a function of cycling. The inset shows the capacity loss for the first cycle as a function of the V/Cu ratio.

4. Conclusions

The incorporation of small amounts of vanadium atoms in copper oxide films allowed the obtention of films with more stable structures in what concerns its ability to react with lithium ions, if compared to the pure copper oxide film. In the mixed oxide films, copper is present in the oxidation state +2 and vanadium in the oxidation state +5. The crystalline structure of the films looses the preferential orientation and become amorphous with the increase of the vanadium content. The capacity loss of the mixed oxides with composition close to that of copper oxide is ∼3 times lower than the capacity loss of the pure oxide, in the second cycle. The oxides also presented a high discharge capacity, specially the film with composition $V_{0.17}CuO_{1.60}$ (CuV60) which presented a capacity ∼563 μAh cm^{-2} μm^{-1} (1042 mAh g^{-1}) in the first cycle.

Acknowledgements

The authors thank CAPES (Brazil) for financial support. Dr. Airton Lourenço is also acknowledged for his help in the experiments. The XANES experiments were performed at the Laboratório Nacional de Luz Síncrotron (LNLS, Campinas, Brazil).

References

[1] M. Lenglett, K. Kartouni, J. Machefert, J.M. Claude, P. Steinmetz, E. Beauprez, J. Heinrich, M. Celati, Mater. Res. Bull. 30 (1995) 393–403.
[2] D.E. Mencer, M.A. Hossain, J.R. Parga, D.L. Cocke, J. Mater. Sci. Lett. 21 (2002) 125–127.
[3] www.webelements.com.
[4] C.A. Vincent, B. Scrosati, Modern Batteries. An Introduction to Electrochemical Power Sources, second ed., John Wiley & Sons Inc.,1997.
[5] D. Linden, Handbook of Batteries, second ed., McGraw-Hill, USA, 1995.
[6] N. Eda, T. Fujii, H. Koshima, A. Morita, H. Ogawa, J. Power Sources 20 (1987) 119–126.
[7] S. Grugeon, S. Laruelle, R. Herrera-Urbina, L. Dupont, P. Poizot, J.-M. Tarascon, J. Electrochem. Soc. 148 (2001) A285–A292.
[8] B. Laik, P. Poizot, J.-M. Tarascon, J. Electrochem. Soc. 149 (2002) A251–A255.
[9] E.A. Souza, R. Landers, L.P. Cardoso, T.G.S. Cruz, M.H. Tabacniks, A. Gorenstein, J. Power Sources 155 (2006) 358–363.
[10] X.P. Gao, J.L. Bao, G.L. Pan, H.Y. Zhu, P.X. Huang, F. Wu, D.Y. Song, J. Phys. Chem. B 108 (2004) 5547–5551.
[11] RUMP/GENPLOT, Computer Graphics Service, 2002.
[12] M.C. Hsiao, H.P. Wang, Y.W. Yang, Environ. Sci. Technol. 35 (2001) 2532–2535.
[13] W.H. Smyrl, S. Passerini, M. Giorgetti, F. Coustier, M.M. Fay, B.B. Owens, J. Power Sources 97–98 (2001) 469–472.
[14] S. DeBeer, C.N. Kiser, G.A. Mines, J.H. Richards, H.B. Gray, E.I. Solomon, B. Hedman, K.O. Hodgson, Inorg. Chem. 38 (1999) 433–438.
[15] M. Takemoto, H. Ikawa, N. Ohashi, T. Ohyama, T. Tsurumi, O. Fukunaga, J. Tanaka, A. Watanabe, Physica C 302 (1998) 151–158.
[16] S.R. Sutton, J. Karner, J. Papike, J.S. Delaney, C. Shearer, M. Newville, P. Eng, M. Rivers, M.D. Dyar, Geochim. Cosmochim. Acta 69 (2005) 2333–2348.
[17] http://www.lasurface.com.
[18] M. Benmoussa, E. Ibnouelghazi, A. Bennouna, E.L. Ameziane, Thin Solid Films 265 (1995) 22–28.
[19] J. Ghijsen, L.H. Tjeng, J. Van Elp, H. Eskes, J. Westrink, G.A. Sawatzky, M.T. Czyzyk, Phys. Rev. B 38 (1988) 11322–11330.
[20] J. Mendialdua, R. Casanova, Y. Babaux, J. Electron Spectrosc. Relat. Phenom. 71 (1995) 249–261.
[21] A.M. Salvi, M.R. Guascito, A. DeBonis, F. Simone, A. Pennisi, F. Decker, Surf. Interface Anal. 35 (2003) 897–905.
[22] Q.-H. Wu, A. Thiben, W. Jaegermann, Solid State Ionics 167 (2004) 155–163.
[23] Q.-H. Wu, A. Thiben, W. Jaegermann, Surf. Sci. 578 (2005) 203–212.
[24] P. Podhajecky, B. Scrosati, J. Power Sources 16 (1985) 309–317.
[25] A. Débart, L. Dupont, P. Poizot, J.-B. Leriche, J.M. Tarascon, J. Electrochem. Soc. 148 (11) (2001) A1266–A1274.
[26] E.A. Souza, R. Landers, M.H. Tabacniks, L.P. Cardoso, A. Gorenstein, Electrochim. Acta, in press.
[27] A. Débart, L. Dupont, P. Poizot, J.-B. Leriche, J.M. Tarascon, J. Electrochem. Soc. 148 (11) (2001) A1266–A1274.
[28] W.H. Smyrl, S. Passerini, M. Giorgetti, F. Coustier, M.M. Fay, B.B. Owens, J. Power Sources 97–98 (2001) 469–472.